Title

EXPERIMENTAL AND PREDICTED OVERALL HEAT TRANSFER COEFFICIENTS FOR FOUR RESIDENTIAL AIR TO AIR HEAT EXCHANGERS

Authors

Seban, R.A.
Rostami, A.
Zarringhalam, M.

Publication Date

1981-12-01

LBL-14448
UC-95d

Lawrence Berkeley Laboratory
UNIVERSITY OF CALIFORNIA

ENERGY & ENVIRONMENT DIVISION

EXPERIMENTAL AND PREDICTED OVERALL HEAT TRANSFER COEFFICIENTS FOR FOUR RESIDENTIAL AIR TO AIR HEAT EXCHANGERS

R.A. Seban, A. Rostami, and M. Zarringhalam

December 1981

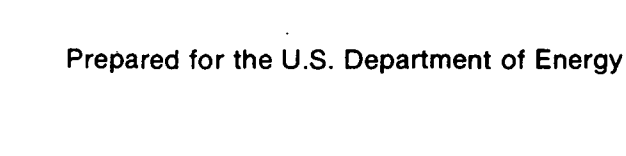

Prepared for the U.S. Department of Energy under Contract DE-AC03-76SF00098

DISCLAIMER

LBL- 14448
EEB-Vent 82-6

Experimental and Predicted Overall Heat Transfer Coefficients for Four Residential Air to Air Heat Exchangers

R.A. Seban, A. Rostami, and M. Zarringhalam

Department of Mechanical Engineering
University of California, Berkeley
Berkeley, California 94720

for

Lawrence Berkeley Laboratory
University of California
Berkeley, California 94720

December 1981

Prepared under UCLBL P.O. No. 7191600 for: The Energy Efficient Buildings Program, Energy and Environment Division, Lawrence Berkeley Laboratory. Principle Investigators: Dave Grimsrud, Craig Hollowell, and Arthur Rosenfeld.

This work was supported by the Assistant Secretary for Conservation and Renewable Energy Office of Buildings and Community Systems, Buildings Division of the U.S. Department of Energy under Contract No. DE-AC03-76SF00098.

Experimental and Predicted Overall Heat Transfer Coefficients for Four Residential Air to Air Heat Exchangers

by

R. A. Seban, A. Rostami, and M. Zarringhalam

Prepared by the
Department of Mechanical Engineering
University of California at Berkeley
under LBL P.O. 7191600

Abstract

Experimental values of the overall heat transfer coefficient are obtained from measured values of the effectiveness for four residental size air-to-air heat exchangers. Predictions of the overall heat transfer coefficient are made from available information, primarily analytical, that specifies the local heat transfer coefficients for the two air streams. For the range of flow rates involved in the experiments, typical of the use of these exchangers, the usual transition criteria imply that the flows are laminar. The correspondence between the experimental and the predicted values of the overall heat transfer coefficients is not very good. Comments are made about these discrepancies, but the differences cannot be definitely explained at present.

Nomenclature

A	transfer area
c	specific heat
c_f	friction coefficient
C	capacity rate
D_h	hydraulic diameter
h	heat transfer coefficient
k	thermal conductivity
ℓ	exchanger length in flow direction
$\dot{m}$	mass flow rate
n_p	number of flow channels
P	channel perimeter
q	heat flux
r_w	thermal resistance of exchanger wall
s	humid heat (specific heat accounting for vapor content of air)
T	temperature
u	mean velocity
U	overall heat transfer coefficient
x	distance in flow direction
y	distance in flow direction, second stream in cross flow exchanger
α	thermal diffusivity
δ	thickness of exchanger wall
η	effectiveness
λ	longitudinal conduction parameter

μ dynamic viscosity

ν kinematic viscosity

ρ density

Subscripts

C cold fluid

H hot fluid

I inlet

O outlet

Superscripts

$\overline{\quad}$ average over exchanger transfer surface

$+$ non-dimensional distance $x^+ = \frac{x}{D_h} \frac{\alpha}{uD_h}$

1. Introduction

Heat exchangers are available commercially for the minimization of the heat losses associated with building ventilation by using the rejected air to heat (in winter) or cool (in summer) the supply of ventilating air by heat transfer from the air withdrawn from the enclosure to be ventilated. These units are composed of a core contained in a case which incorporates the inlet and outlet fittings, and which case may enclose also blowers for air induction and rejection, together with the motors that drive the blowers. The case contains a drain for condensate removal, since condensation may occur on the side of the hot air stream if conditions are such that the temperature of the transfer surface at any location falls below the dew point temperature of the entering hot stream.

Tests have been made to determine the effectiveness of such exchangers under conditions in which condensation did not occur, and Fisk, et al. (1) have given the effectiveness as a function of the flow rate for five such exchangers. These were of relatively small size, as intended for domestic use. In those units which incorporated blowers, these were either removed or were inoperative. In addition to the effectiveness, Ref. (1) gives complete details of the test system and of the exchangers and also gives information on the pressure drop measured across them.

This report is concerned with the evaluation of the overall heat transfer coefficient from the measured values of the effectiveness and with the prediction of this coefficient to determine how well the experimental and the predicted coefficients compare. This evaluation is made for four of the exchangers for which results are given in Ref. 1. No appraisal of experimental and predicted pressure drops is made in this report because, in general, the pressure drop in the case, external to the core, is large compared to the pressure drop in the core itself.

The purpose of this comparison of the experimental and the predicted overall heat transfer coefficient was to establish the predictive capacity of the models for the local transfer coefficients for the hot and cold air sides of the exchanger. This appraisal is valuable in respect to exchanger design and also in respect to the further problem of performance prediction for operating conditions in which condensation or freezing may occur within the exchanger.

2. The Exchangers

Two of the exchangers are cross flow units, and are made of aluminum sheets, to produce a basic flow channel which is essentially a rectangle of large aspect ratio. One, the Genvex VMC exchanger, hereafter referred to as the G exchanger, has precisely this flow cross section, identical for each of the hot and cold streams. Table 1 gives the essential dimensions of this exchanger, and of the other three exchangers as well. The other cross flow exchanger, the Flakt RDAA exchanger, hereafter referred to as exchanger F, is of the same basic geometry as exchanger G, but contains between the parallel plate surfaces which separate the hot and cold streams a corrugated aluminum sheet, which sheet is not bonded to the parallel surfaces. This corrugated sheet provides a parallel system of roughly triangular flow passages, of the form indicated on Fig. 1. The sheet produces fins on the basic surfaces, with a fin effectiveness that depends in magnitude on the contact resistance at the lines on which the corrugations touch the parallel plates.

The other two exchangers considered here are counterflow units. One was a unit fabricated according to the design of a unit available commercially (2). Here this exchanger is referred to as exchanger B. The transfer surfaces were plastic sheets, separated at the exchanger edges by 1.9 cm (.75 in) thick

wood strips, that also formed the exterior of opposite sides of this exchanger. The enclosure is completed by plywood sides parallel to the plastic sheets that formed the case. The hot air enters the top and leaves at the bottom, and the cold air enters the side, near the bottom, through a gap in the spacers. The cold air leaves through a similar gap on the opposite side, near the top of the exchanger. Thus, the flow is counterflow through most of the core length, but it departs from this configuration near the top and near the bottom.

The fourth exchanger, also a counterflow unit, is an Aldes VMPI exchanger, hereafter this exchanger is denoted as exchanger A. It is made of a stack of stiff plastic sheets. These sheets are of a rectangular plan form with triangular ends. In the central rectangular section, as shown on Fig. 1, these sheets are corrugated in such a way that the contact of two adjacent sheets produces flow cross-sections of rhombic form, (a diamond shaped cross-section) with alternate hot and cold channels. The corrugations are different on the triangular ends, where the sheets have localized corrugations that, projecting against the adjacent sheet, produce a number of rectangular channels through which the hot air (for one pair of sheets) or the cold air (for the adjacent pair of sheets) is directed to the hot and cold channels formed by the corrugations as defined above. Within the central part of the core region, the cold air passages are changed to a triangular form by a flat plastic sheet placed between the corrugated sheets, as shown on Fig. 1. A stack of such sheets forms the core, and registration is maintained by the outer case of the exchanger.

3. The Experimental Effectiveness

The tests were made to determine the effectiveness. In them the ratio of the capacity rates C_H/C_C, i.e., $(\dot{m}_H s)/(\dot{m}_H s)$, ranged from 0.93 to 0.98, with

hot air inlet temperatures between 21°C (70°F) and 27°C (80°F) and cold air inlet temperatures between 10°C (50°F) and 7°C (45°F). Hot air was supplied and returned through a loop that contained heaters, fan, orifice meters for the inlet and outlet flows and thermocouple rakes for the measurement of the mean temperatures, these rakes being immediately adjacent to the inlet and outlet fittings on the exchanger case. The cold air circuit was similar, except for the incorporation of cooling coils. Pressure adjustments were available so that the pressure at the hot air inlet and cold air inlet could be equalized.

In operation, for all of the exchangers, the balance between the total inflow, $\dot{m}_{HI} + \dot{m}_{CI}$, and the total outflow, was generally within 1%, and the individual balances, as between hot air inflow, $\dot{m}_{HI}$ and the hot air outflow, $\dot{m}_{HO}$, were also relatively close. Other evidence revealed that leakage may have occurred in the case, between the hot air into the core and the cold air out of the core, and similarly between the cold air in and the hot air out. Such leakage, if it occurred, had the consequence of increasing the effectiveness, as measured from the temperatures that were observed outside of the exchanger case, above the true value associated with the core itself. Significant leakage of this type probably did occur with the G exchanger.

Tests were made for a range of flow rates from about 0.023 m^3/sec (50 ft^3/min) to 0.118 m^3/sec (250 ft^3/min), and numerous tests were made for any given operating conditions. Comparison of the energy loss from the hot stream, $Q_H = s(\dot{m}_{HI}T_{HI} - \dot{m}_{HO}T_{HO})$, to the gain by the cold stream $Q_C = s(\dot{m}_{CO}T_{CO} - \dot{m}_{CI}T_{CI})$ indicated significant uncertainty in the rate of heat transfer. With the "loss" specified as $Q_H - Q_C = Q_L$, the ratio $\frac{Q_L}{Q_H}$ varied substantially, and it could not be rationalized in terms of any logical heat transfer from the exchanger case. Therefore, there were selected for

evaluation only those runs for which $\left|\frac{Q_L}{Q_H}\right|$ was a minimum, and even with this selection, the ranges of $\frac{Q_L}{Q_H}$ were, for exchanger G, $0.0 < \frac{Q_L}{Q_H} < 0.14$; for exchanger F, $-0.07 < \frac{Q_L}{Q_H}$ 0.02; for exchanger B, $-0.01 < \frac{Q_L}{Q_H} < 0.10$, and for exchanger A, $-0.04 < \frac{Q_L}{Q_H} < 0.07$. Few runs were made with Exchanger B because there was difficulty in maintaining stable operating conditions. Apparently the core pressure drops were affected by motion of the thin plastic sheets, despite attempts that were made to maintain nearly equal pressures in the hot and cold air streams.

Figure 2 shows the effectiveness for the four exchangers, one point being shown on that figure for each flow rate, the point being selected on the basis of the best energy balance. For both the G and the F, counterflow exchangers, the hot air effectiveness, $\eta_H = (T_{HI} - T_{HO})/(T_{HI} - T_{CI})$ and the cold air effectiveness, $\eta_c = (T_{CO} - T_{CI})/(T_{HI} - T_{CI})$, were both evaluated. For a capacity rate ratio, C_H/C_C, less than unity, the former should be compared to the mass rate of flow of the hot air. For the ultimate evaluation of the overall heat transfer coefficient, however, almost the same coefficient will be evaluated if the average effectiveness, $\eta_A = (\eta_H + \eta_C)/2$ is compared to the average inflow rate, $(\dot{m}_{HI} + \dot{m}_{CI})/2$, when the two flow rates are as nearly equal as they were in the present experiments. The results for the G exchanger, because of their erratic nature, required this representation to secure consistency, and for both exchangers this interpretation was required for the evaluation of an overall heat transfer coefficient because of limitations on the analytical information that is available for the evaluation of the effect of longitudinal conduction, which was important in these exchangers. Thus for the G and F exchangers, Fig. 2 shows η_A as a function of $(\dot{m}_{HI} + \dot{m}_{CI})/2$.

For the counterflow exchangers, exchangers B and A, Fig. 2 shows, as points, the hot side effectiveness, η_H, as a function of $\dot{m}_{HI}$, the mass flow rate of the inlet hot air stream.

Figure 2 contains curves drawn as an estimate of the possible form of the function $\eta = f(\dot{m})$. Analytical considerations indicate that if the overall transfer coefficient is constant, or increases monotonically with flow rate, that the negative slope of the relation, $\eta = f(\dot{m})$, should increase monotonically with "$\dot{m}$" increasing. The pictured curves conform to this. The curves themselves, the best estimate of $\eta = f(\dot{m})$, are not used otherwise in this report.

4. The Experimental Overall Heat Transfer Coefficient

For the cross flow exchangers, in which longitudinal conduction was significant, the relation between the effectiveness and the overall heat transfer coefficient is obtained from the results of a numerical computation. This gives the effectiveness in terms of the Number of Transfer Units, UA/C_H, where the overall transfer coefficient is assumed to be invariable over the exchanger area, and the ratio of the capacity rates, C_H/C_C and the quantities, λ_H and λ_C, associated with the longitudinal conduction in the two flow directions. The quantity λ is $n_P\ k_m\ \delta_m/C$, where n_P is the total number of flow passages, k_m is the conductivity of the metal, and δ_m is the effective thickness of the metal wall, per passage. For the G exchanger, with parallel walls, δ_m is the wall thickness. For the F exchanger, it is an effective value evaluated from the wall thickness and the length of the corrugation thickness per unit wall width. Chiou (3) has given results that can be translated to $\eta_H = f(\frac{U_A}{C_H}, \frac{C_H}{C_C}, \lambda_H, \lambda_C)$ but, in terms of the present range of capacity rates, those results are available only for $\eta = f(\frac{U_A}{C}, \lambda)$, for

equal capacity rates and, as in the G and F exchangers, equal λ values for both flow directions. (These results were, in fact, confirmed by separate numerical calculations, done in a slightly different way from that described in Ref. (3), for a restricted range of λ and $\frac{UA}{C}$. The incentive for such a calculation was an initial view that Ref. (3) might be wrong; in fact the results of that reference were confirmed.)

Figure 3 is a picture of the relation $\eta = f(\frac{UA}{C}, \lambda)$ for equal capacity rates. A logarithmic representation is used on this picture to achieve a better illustration. To evaluate the number of transfer units, $\frac{UA}{C}$, however, a Cartesian plot of these results, incorporating more curves for different λ values, was used. For the G exchanger λ is 4.8/C with C in W/°C, (9.41/C) with C in Btu/hr°F, and for the F exchanger this value is 2.8/C (or 5.4/C), the numerator being smaller for the F exchanger because the effective thickness δ is smaller, even with the corrugated sheet between the plates, because of the thinner aluminum sheet used in the fabrication of this exchanger. At the lowest flow rates, λ is 0.124 for the G exchanger and 0.09 for the F exchanger; at the highest flow rates these two values are 0.03 and 0.02, respectively.

For any effectiveness, given as a point on Fig. 2, for a given flow rate, λ can be evaluated. Then for this η and λ, interpolating if necessary on the plot of $\eta = f(\frac{UA}{C}, \lambda)$, the Number of Transfer Units is specified. From it, given the capacity rate and the specified transfer area, the overall coefficient, U, is determined. These coefficients are shown as points on Fig. 4, based on the plate area of 8.64 m^2 (93 ft^2) for the G exchanger and the combined area of the plates and the corrugated sheets of 19.8 m^2 (213 ft^2) for the F exchanger.

The Reynolds number $\frac{4\dot{m}}{P\mu}$, where P is the total flow perimeter, ranged from about 350 to 1700 for the G exchanger and from about 100 to 425 for the F

exchanger. These are approximate evaluations based on the average temperature of the air streams, they are actually slightly lower on the hot side and slightly higher on the cold side. But laminar flow is indicated for both streams, and the substantial dependence of the overall transfer coefficient on the flow rate that is indicated on Fig. 3 is surprising, and, as is subsequently shown, this cannot be rationalized at the present time.

Both the B and the A exchanger are partly cross flow at the ends, and the nature of this cross flow is such that the prediction of an effectiveness relation, $\eta_H = f(\frac{UA}{C_H}, \frac{C_H}{C_C})$, would be a substantial task. Rather, complete counterflow was assumed, even though it did not really exist. Also, because of the relatively low conductivity of the plastic which formed the transfer surfaces, longitudinal conduction was not important in these exchangers. Under these circumstances, the transfer units $\frac{\overline{U}A}{C_H}$, where $\overline{U}$ is the average of the overall transfer coefficient for the exchange area, were not evaluated from the experimental effectiveness values as shown on Fig. 2 but were evaluated from the terminal temperatures as:

$$\frac{\overline{U}A}{C_H} = \frac{T_{HI} - T_{HO}}{(\Delta T)_{\ell m}} \qquad (1)$$

Here $(\Delta T)_{\ell m}$ is the logarithmic mean of the terminal temperature differences, or, for capacity rate ratios close to unity, this is the arithmetic mean of the terminal temperature differences. Figure 5 shows by points the values of $\overline{U}$ obtained in this way, based on a transfer area of 19.2 m^2 (208 ft^2), the sheet area for the B exchanger, and of 19.1 m^2 (205 ft^2), the total area of the corrugated sheets, for the A exchanger.

The Reynolds number, $\frac{4\dot{m}}{P\mu}$, ranged from about 665 to 2800 in the B exchanger. In the A exchanger the Reynolds number varied in the different flow cross-sections because of the different perimeters of the different flow cross-sections; the high and low values for each are given approximately in the following tabulation.

Flow Section	Rectangular	Rhombic	Triangular
Low Reynolds	750	370	250
High Reynolds	3600	1760	1200

5. Predictions of the Overall Heat Transfer Coefficient

The prediction of the overall heat transfer coefficient requires the specifications of the local heat transfer coefficients for the hot and the cold air streams. These local coefficients are given in terms of a Nusselt Number, which in general depends upon the Reynolds Number, the Prandtl Number, and a distance from the position at which heat transfer begins. This distance dependence is associated with the hydrodynamic and thermal development in the initial region, a domain often called the entry length. Ultimately there is attained an asymptotic regime in which the Nusselt number is essentially constant. Entry lengths of this nature also occur if the channel cross section or the temperature of the channel walls change abruptly.

In the present analysis, only thermal effects are considered for the specification of the variation of the local coefficient in the entry length. For the exchangers and the flow rates associated with them, the flows have been indicated to have been primarily laminar, and the local heat transfer coefficient for the entry length is approximated by the Leveque-Lighthill solution. This is adopted up to the position at which the heat transfer coefficient that it gives is equal to the separately known analytical results for

the asymptotic value of the heat transfer coefficient. For flow situations for which an exact solution is known, this kind of specification is precise for small and for large distances from the point at which heating begins, and is only slightly low in the region near the termination point of the Leveque-Lighthill solution.

The coefficient, as given by the Leveque-Lighthill solution, depends on the nature of the temperature or heat flux variation in the direction of flow. For the cross flow exchangers the solution for a constant overall coefficient, on which the effectiveness specification is based, indicates a variation of wall temperatures, with flow direction, that varies across the span of the exchanger. Inspection of that solution, however, indicates that the local heat flux tends to be reasonably constant over the exchanger area when the ratio of the capacity ratio is nearly unity. Therefore, there is used the form of the Leveque-Lighthill solution associated with a constant value of the quantity $q/\left(\rho c u \sqrt{\frac{c_f}{2}}\right)$. If the hydrodynamic entrance effect is neglected, so that the friction coefficient is constant, this corresponds to a constant heat flux. The solution is then:

$$\frac{q}{\rho c u \sqrt{\frac{c_f}{2}}} = \frac{0.645\ (T_W - T_M)}{\left(\frac{\nu}{\alpha}\right)^{2/3} \left[\frac{ux}{\nu} \sqrt{\frac{c_f}{2}}\right]^{1/3}} \qquad (2)$$

In this equation $(T_W - T_M)$ is the excess of the wall over the fluid mean temperatures. It is to be recalled that in the derivation of Eq. 2 it was assumed that T_M was constant. While this is not true in the channel flow that is considered, the result, Eq. 2, is still a reasonable approximation to the exact solution in the region in which the local heat transfer coefficient, $h = q/(T_W - T_M)$, is variable.

For constant wall temperatures, the numerical coefficient in Eq. 2 is 0.534 instead of 0.645. The ratio of these is 1.20, and this is the ratio between the indicated heat transfer coefficients for constant heat flux and for constant wall temperature. In the application to the cross flow heat exchanger, the uncertainty about the predicted local coefficient may be in this range.

The friction coefficient for fully developed laminar flow is given as $(\frac{UD_h}{\nu})\frac{c_f}{2} = N$, where N is a number depending in magnitude on the channel geometry. If this specification is introduced into Eq. 2, then this equation takes the form:

$$\frac{hD_h}{k} = \frac{0.645\ (N)^{1/3}}{\left[\frac{x}{D_h}\ \frac{\alpha}{u\ D_h}\right]^{1/3}} = \frac{0.645\ (N)^{1/3}}{\left[x^+\right]^{1/3}} \tag{3}$$

This local coefficient equals the known asymptotic coefficient, h_∞, at the location $x^+ = \xi^+$, and the transfer coefficient is taken as its asymptotic value for $x^+ > \xi^+$. Therefore the average coefficient in the length ℓ^+, $\ell^+ > \xi^+$, is given as:

$$\frac{hD_h}{k} = \frac{1}{\ell^+}\left[\int_0^{\xi^+} (\frac{hD_h}{k})\, dx^+ + (\frac{h_\infty D_h}{k})\ (\ell^+ - \xi^+)\right] \tag{4}$$

From Eq. 3

$$\int_0^{\xi^+} \frac{hD_h}{k}\, dx^+ = 1.5 \left(\frac{hD_h}{k}\right)_{\xi^+} \xi^+$$

where $\left(\frac{hD_h}{k}\right)_{\xi^+}$ is the value at ξ^+, which is $\frac{h_\infty D_h}{k}$. Therefore:

$$\frac{\bar{h}D_h}{k} = \frac{1}{\ell^+}\left[1.5\left(\frac{h_\infty D_h}{k}\right)\xi^+ + \left(\frac{h_\infty D_h}{k}\right)(\ell^+ - \xi^+)\right]$$

or

$$\frac{\bar{h}D_h}{k} = \frac{h_\infty D_h}{k}\left(1 + 0.5\,\frac{\xi^+}{\ell^+}\right)$$

The values of N and of $\frac{h_\infty D_h}{k}$ are given by Shah and London (4) for a large variety of flow channels. For the G and B exchangers, the parallel plate values were used; for the F exchanger a triangular cross section of the dimensions indicated on Fig. 1 was chosen (a sinusoidal form having the amplitude and wavelength indicated by those dimensions does not lead to very different results). For the A exchanger, there were used the triangle and rhombus approximations, and the rectangular channel approximation, made on the basis of the dimensions that are shown on Fig. 1. The tabulation that follows gives the values of $\mathrm{Re}\,\frac{c_f}{2}$ and $\frac{h_\infty D_h}{k}$, for the constant heat rate case, from Ref. (4), and the value of ξ^+ that is obtained from the match of $\frac{hD_h}{k}$ from Eq. 3 and the value of $\frac{h_\infty D_h}{k}$.

Table II

	$Re \frac{c_f}{2}$	$\frac{h_\infty D_h}{k}$	ξ^+
Parallel Plates, G,B	12	8.23	0.020
Triangular, F	6.60	3.05	0.064
Triangular, A	6.65	2.75	0.090
Rhombic, A	7.02	3.70	0.038
Rectangular, A	9.12	5.33	0.048

For the G exchanger, the cross flow parallel plate unit, the local overall heat transfer coefficient is:

$$\frac{1}{U} = \frac{1}{h_H} + \frac{1}{h_c} + r_w \tag{5}$$

and the average for the exchanger area, A = LW (for the G exchanger L = W) is

$$\overline{U} = \frac{1}{A}\int_0^L \int_0^W \frac{1}{\left(\frac{1}{h_H} + \frac{1}{h_c} + r_w\right)} \, dx \, dy \tag{6}$$

This complicated integration was not carried out. For the G exchanger, in fact, the ratio, ξ^+/ℓ^+ is always relatively small, and over most of the area the local transfer coefficients equal their asymptotic value, h_∞. Thus, an approximation is to evaluate the average coefficients for each side of the exchanger from Eq. (4) and to then approximate the average overall coefficient as:

$$\frac{1}{\overline{U}} = \frac{1}{\overline{h_H}} + \frac{1}{\overline{h_c}} + r_w \qquad (7)$$

The resistance of the metal exchanger wall is negligible compared to the other two terms on the right side of Eq. 7. While the coefficients $\overline{h}_H$ and $\overline{h}_c$ differ because of differences in the properties of the average temperature of the hot and cold streams, the difference is not great, and it is appropriate to evaluate both h_H and h_c at the average air temperature. Then $\overline{h}_H \approx \overline{h}_c$, since the hot and the cold flow rates are almost the same. On this basis $\overline{U} = \overline{h}/2$. This result is shown as a line on Fig. 4. There is very little variation of $\overline{U}$ with mass flow rate because the thermal entry region ($x^+ < \xi^+$) is so small for this exchanger.

For the F exchanger, the cross flow unit with the corrugated metal insert between the parallel plates, the specification of U depends upon the effectiveness of the fins that are produced by the corrugated insert. If negligible resistance is assumed for the contact between the corrugation and the plates that separate the streams, then the magnitude of the predicted heat transfer coefficients, the fin thickness, and the conductivity of this aluminum insert, are such as to make the fin effectiveness essentially equal to unity. Then the entire periphery of the small channel formed by the corrugation and the parallel walls is at essentially constant temperature, and the effective transfer area is defined by the channel periphery. The local overall heat transfer coefficient is then based on this area. For the F exchanger the values of ξ^+/ℓ^+ are of the same order as they are for the G exchanger. Again the procedure associated with Eq. 7 was used to give the result for $\overline{U}$ that is indicated on Fig. 4.

For the counterflow exchangers, exchangers B and A, there is less ambiguity about the experimental value as deduced from Eq. 1 because for a truly counterflow case the number of transfer units is truly $\overline{U}A/C_H$. The predicted average coefficient is:

$$\overline{U} = \frac{1}{\ell} \int_0^{\ell} \frac{1}{\left(\frac{1}{h_H} + \frac{1}{h_c} + r_w\right)} \, dx \tag{8}$$

For these exchangers, the resistance, r_w, of the plastic walls is still far less than the value of $(1/h_H + 1/h_c)$ and it can be neglected. Also, for the counterflow exchanger, if the capacity rates are equal the temperature difference between the two streams is constant. The capacity rate ratio was indeed nearly unity, but the local heat flux still varies in proportion to the change in the local value of the overall heat transfer coefficient. Considering that this variation is not too great, the application of Eq. 3, and a value of h_∞ corresponding to constant heat rate, is justifiable.

The value of ξ^+/ℓ^+ for the B exchanger is so small that the coefficients on the hot and the cold side are almost constant over the whole length of the exchanger, thus the average overall coefficient is given to a good approximation by Eq. 8. For the counterflow exchanger, the application of Eq. 8 is also supported by the analysis of Seban, et al. (5). Figure 5 shows by a line the value of $\overline{U}$ predicted for the B exchanger. The thermal entry effect is so small that the predicted value of $\overline{U}$ is almost invariable with the flow rate.

The prediction of the overall transfer coefficient for exchanger A is complicated by the changes in flow cross section in the exchanger length. For the hot air side this involves the change from the rectangular cross section at the inlet to the long rhombic section, and then the change to the rectangular

section at the outlet. For the cold air side the rhombic section is further changed to the triangular cross section in the central part of the exchanger. Clearly, there is a hydrodynamic effect at each point at which the flow section changes, and at these locations there is a concomitant change in the temperature distribution across the flow cross section. In the prediction, the hydrodynamic effects, which are in any case unknown, were ignored, and it was assumed that at each cross section the temperature distribution across the flow area became completely uniform, at the local mixed mean temperature.

Equation 8 was used to evaluate the mean heat transfer coefficient, with the local heat transfer coefficients evaluated from Eq. 3 with x^+ measured from the location of the last change in flow cross section, and as h_∞ for $x^+ > \xi^+$. This calculation was only made for the lowest and for the highest flow rate. For the highest flow rate the Dittus-Boelter equation

$$\frac{hD_h}{k} = .023 \left(\frac{uD_h}{\nu}\right)^{0.8} \left(\frac{\nu}{\alpha}\right)^{0.4} \tag{9}$$

was used for the evaluation of the local coefficients in the rectangular cross sections at the ends of the exchanger because there the Reynolds number, as noted in Section 4, substantially exceeded 2000. Thus no thermal entry effect was considered for these sections.

While on the basis of this calculation of $\bar{U}$, there is not a linear relation between $\bar{U}$ and the flow rate, there is shown on Fig. 5 a straight line that connects the two extreme values of $\bar{U}$ that were calculated.

6. An Appraisal of the Predictions

Views of Figs. 4 and 5 have already indicated that the predictions, always made somewhat approximately but nevertheless with some care, are

relatively far from the experimental values. Particularly when the experimental values are lower than the predicted values, the following discussion of other possible effects does not indicate definitely any effects which serve to rationalize this kind of discrepancy.

For the G exchanger, the experimental coefficients are close to the predicted coefficients only at the highest flow rate, otherwise they are lower. In this regard it can be noted that the effect of longitudinal conduction was most important at the lowest flow rate, and its use as specified earlier produced at the lowest flow rate the experimental transfer coefficient of 10.3 $W/m^2°C$ (1.82 Btu/hr $ft^2°F$) that is shown on Fig. 4. Had the effect of conduction been neglected ($\lambda = 0$), the experimental value deduced from Fig. 3 would have been 7.26 $W/m^2°C$ (1.28 Btu/hr $ft^2°F$). The suspicion that the evaluation of the effect of longitudinal conduction that is specified by Fig. 3 might be too small led to the check of that result that was already mentioned. Actually, the very complicated evaluation which would account for the variable coefficients in the thermal entry regime would need to be made to appraise longitudinal conduction effects under these conditions. For the G exchanger, however, the entry length region is so small that the evaluation from Fig. 3 is probably appropriate.

In the test of the G exchanger, its orientation was such that the hot air flow was diagonally upward and the cold air flow was diagonally downward. For such a situation any free convection effects would, by theory, tend to diminish the heat transfer coefficient. But experiments by Mullin and Gerhard (6), made for liquid flow in a tube under such conditions, but confined to the thermal entry region, produced an opposite effect. Here it is noted only that a Grashof number, based on the distance between the plates, and a typical temperature difference of 4°C between the air and the surface is about 25, or

180 if D_h is used as the significant dimension. At the lowest flow rate the Reynolds number, uD_h/ν is about 350. The ratio of the Grashof number to the square of the Reynolds number is usually on the order of unity if free convection effects are to become important; for the G exchanger this ratio is far lower. Thus the low transfer coefficients measured with the G exchanger at all flow rates except the highest are unexplainable on the basis of such an effect.

For the F exchanger the measured values are much lower than the predicted values, as is evident from Fig. 4, but it must be recalled that the prediction was based on zero contact resistance between the corrugated sheet and the wall. A value of that resistance, necessary to bring predicted values into better accord with measurement, can be deduced, but this value is not very significant without some standard of comparison. It can be noted that if this resistance was infinite, then the transfer would be only to the parallel plates. Then that area alone should be used for the prediction of the experimental coefficients and they would be increased by the relevant area ratio which is 2.68. The predicted value of the average overall coefficient for this situation can be based, in terms of available results, only on the case in which the two sides of the triangular section formed by the corrugation would be adiabatic. This would lower slightly the predicted value of $\overline{U}$ from that shown on Fig. 4 for this exchanger. An increase of 2.68 in the experimental coefficient, together with but a slight change in the predicted coefficient, would place the experimental coefficients in considerable excess of the predicted values. This does demonstrate that the corrugation provides a substantial fin effect and that the exchanger performance might possibly be improved by bonding the corrugated sheets to the plates to eliminate the contact resistance that apparently exists there.

For the B exchanger, for which, as noted before, the experimental results are in some question, Fig. 5 indicates that there is some agreement between experimental and predicted transfer coefficients at low flow rates. At higher flow rates, however, the experimental values become substantially larger than the predicted ones. Particularly in view of the instability of the plastic surfaces of this heat exchanger, there is the possibility of an early transition to turbulence. As an appraisal of the possible effect of turbulence, the Dittus-Boeltus relation gives a Nusselt number of 12 for a Reynolds number of 2000, but this is scarcely greater than the laminar flow Nusselt number of 8.23 for the parallel plate case as contained in Table II, so that on the assumption of turbulent flow at the highest flow rate the prediction of $\overline{U}$ would be increased from 2.7 to 3.9 W/m^2C. The experimental value is 5.7 W/m^2C. Reynolds, et al. (7) have noted that the Dittus-Boelter equation apparently holds to a Reynolds Number as low as 3000 in pipe flow, and that this is predictable from a modified form of the Reichardt mixing length expression, actually originally derived from measurements in a channel of large aspect ratio. For the pipe, for which $h_\infty D_h/k$ is 4.35, the assumption of turbulent flow at low Reynolds numbers therefore produces a more substantial increase in the heat transfer coefficient.

It can be noted in this respect that a prediction, made on the basis of the modified mixing length distribution, was actually made numerically for the parallel plate case, to a Reynolds number as low as 2400. The result was not much different than what would be indicated by the use of the Dittus-Boelter equation to Reynolds number as low as this, and the results therefore did not rationalize the discrepancy between the predicted and the experimental values of $\overline{U}$ for the B exchanger.

Besant, et al. (2) quoted results for an exchanger similar to the B exchanger, except that the spacing between the parallel plastic sheets was 1.27 cm instead of the 1.91 cm of the B exchanger. As with the B exchanger, the hot air flowed downward while being cooled and the cold air flowed upward while being heated. With these conditions free convection effects are expected to augment the heat transfer. Besant, et al. indicated such an effect, and they specified their results for the overall heat transfer coefficient by the relation

$$\frac{2\bar{U}D}{k} = 3.6 + 3.4 \times 10^4 \left(\frac{Gr}{Re^2}\right)^2 \qquad (10)$$

Here D is the distance between the plastic sheets and this dimension was used in evaluating the Grashof number. The basis of the evaluation of the Reynolds number is not clear. If the plate spacing is used for D everywhere in Eq. 10 then the overall coefficients predicted from Eq. 10 exceed by far the experimental values for the B exchanger that are shown on Fig. 5. The only present connection that is associated with Eq. 10 is its indication that the overall coefficients rise very substantially at low flow rates. This is completely opposite to the trend of the experimental coefficients that is shown on Fig. 5.

For the A exchanger, as for the B exchanger, Fig. 5 shows some correspondence between predicted and experimental values of $\bar{U}$ only at the lowest flow rates. At about the average of the highest and lowest flow rates, and above, the experimental coefficients are substantially higher than the predicted values. As with the B exchanger, there is the indication of an early transition to turbulence and, for the A exchanger, for which the values of $h_\infty D/k$ in the central core region are relatively low, a substantial increase in the co-

efficient might be expected. As an example, for the highest flow rate, it has been indicated that the Reynolds numbers are about 1730 in the rhombic sections. If the flow in these rhombic sections is assumed to be turbulent, and the local transfer coefficients are obtained from Eq. 9, then the value of U that is calculated from Eq. 8 is 9.3 W/m^2C instead of the value of 6.55 W/m^2C as indicated on Fig. 5. But this prediction is still less than the experimental value of 13.1 W/m^2C, though the trend is acceptable.

In all of the foregoing considerations, it was assumed that the air flows were uniformly distributed amongst the flow channels on both the hot and the cold sides of the exchangers. Some considerations as to the possible effect of non-uniformity in the flow distribution were made, but without any positive conclusion. As a limiting condition, however, it can be noted that for laminar flow conditions in which the thermal entry length is not too significant, say as in Exchanger B, the heat transfer coefficient is independent of the flow rate, and under these conditions the predicted value of the overall coefficient would be relatively independent of the flow distribution.

7. Conclusions

This comparison of experimental and predicted overall heat transfer coefficients for four heat exchangers shows that the predictions, made essentially for laminar flow because the Reynolds numbers were generally below 2000, are but marginally capable of predicting the experimental results. The comparisons indicate a need for: (1) additional heat transfer information on flows with low Reynolds numbers which may be turbulent, and (2) for a further investigation on the effect of the thermal entry length on the prediction of the effectiveness for cross flow heat exchangers, both with and without longitudinal conduction, and (3) further investigation on the effect of free convection under circumstances in which that might be expected to diminish the heat transfer coefficient.

Until more accurate and complete models are developed for the prediction of the heat transfer coefficient, experiments on the actual exchangers are required to establish the performance of the types of exchangers considered here, and the true values of the local heat transfer coefficients must be inferred from this performance.

References

1. Fisk, W.J., Roseme, G.D., and Hollowell, C.D., "Performance of Residential Air to Air Heat Exchangers: Test Results and Methods," Lawrence Berkeley Laboratory. Report, LBL-11793, September 1980.

2. Reference is to an exchanger similar to that obtainable from D.C. Heat Exchangers, Rural Route 3, Saskatoon, Saskatchewan, Canada. Other details are given by a paper "Design of Low Cost Ventilation Heat Exchangers" by R.W. Besant, E.E. Brooks, G.J. Schoenan, and R.S. Durmont, obtainable from the above address.

3. Chiou, J.P., "The Effect of Longitudinal Heat Conduction on the Crossflow Heat Exchanger," Journal of Heat Transfer, Vol. 100, 1978, pp. 346-351.

4. Shah, R.K. and London, A.L., Laminar Flow Forced Convection in Ducts, Advances in Heat Transfer, Academic Press, New York, 1978.

5. Seban, R.A., Hsieh, T.C., and Greif, R., "Laminar Counterflow Exchangers: An Approximate Account of Wall Resistance and Variable Transfer Coefficients," Journal of Heat Transfer, Vol. 94, 1972, p. 391.

6. Mullin, T.E., and Gerhard, E.R., "Heat Transfer to Water in Downward Flow in a Uniform Wall Temperature Tube at Low Graetz Numbers," Journal of Heat Transfer, Vol. 99, 1977, p. 586.

7. Reynolds, H.C., Swearingen, T.B. and McEligot, H.M., "Thermal Entry for Low Reynolds Number Turbulent Flow," Journal of Basic Engineering, Vol. 91, 1969, p. 87.

Acknowledgment

This work was supported by the Assistant Secretary for Conservation and Renewable Energy, Office of Buildings and Community Systems, Buildings Division of the U.S. Department of Energy under Contract No. DE-AC03-76SF00098, and under subcontract No. UCLBL PO NO. 7191600.

TABLE I

HEAT EXCHANGER CORE DIMENSIONS

	Genvex G	Flakt F	(Besant) B	Aldes A
Core Height	16.8	32.2	38.4	140.0
Width cm	47.6	30.5	51.5	41.2
Length cm	47.6	30.5	198.0	24.1
Channel Height cm	0.37	0.37	1.91	See Fig. 1
Width cm	47.6	30.5	51.5	
Hyd. Dia., D_h cm	0.74	.29 see Fig. 1	3.82	
Wall thickness cm	.06	.0075	.015	Fig. 1
Number of Channels				
Hot	19	42	10	32 x 13
Cold	20	43	10	32 x 12
Transfer Area (m^2)	8.64	7.8	19.3	17.3 (central)
Hot to cold interface		+ 12.0 (corrug)		+ 1.7 (triangular ends)
		19.8		19.0

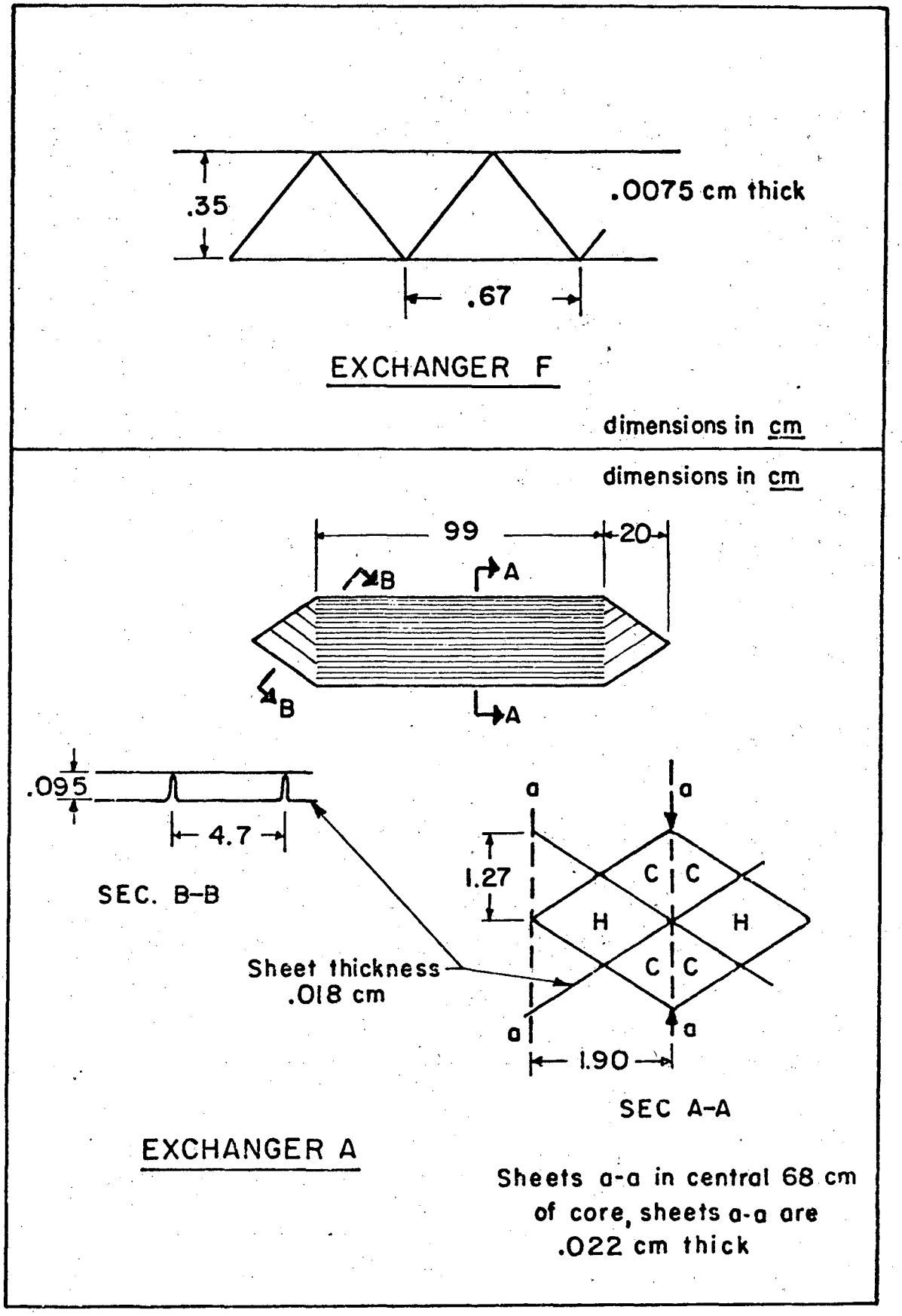

Figure 1. Details of Channels, Flakt, and Aldes Exchangers.

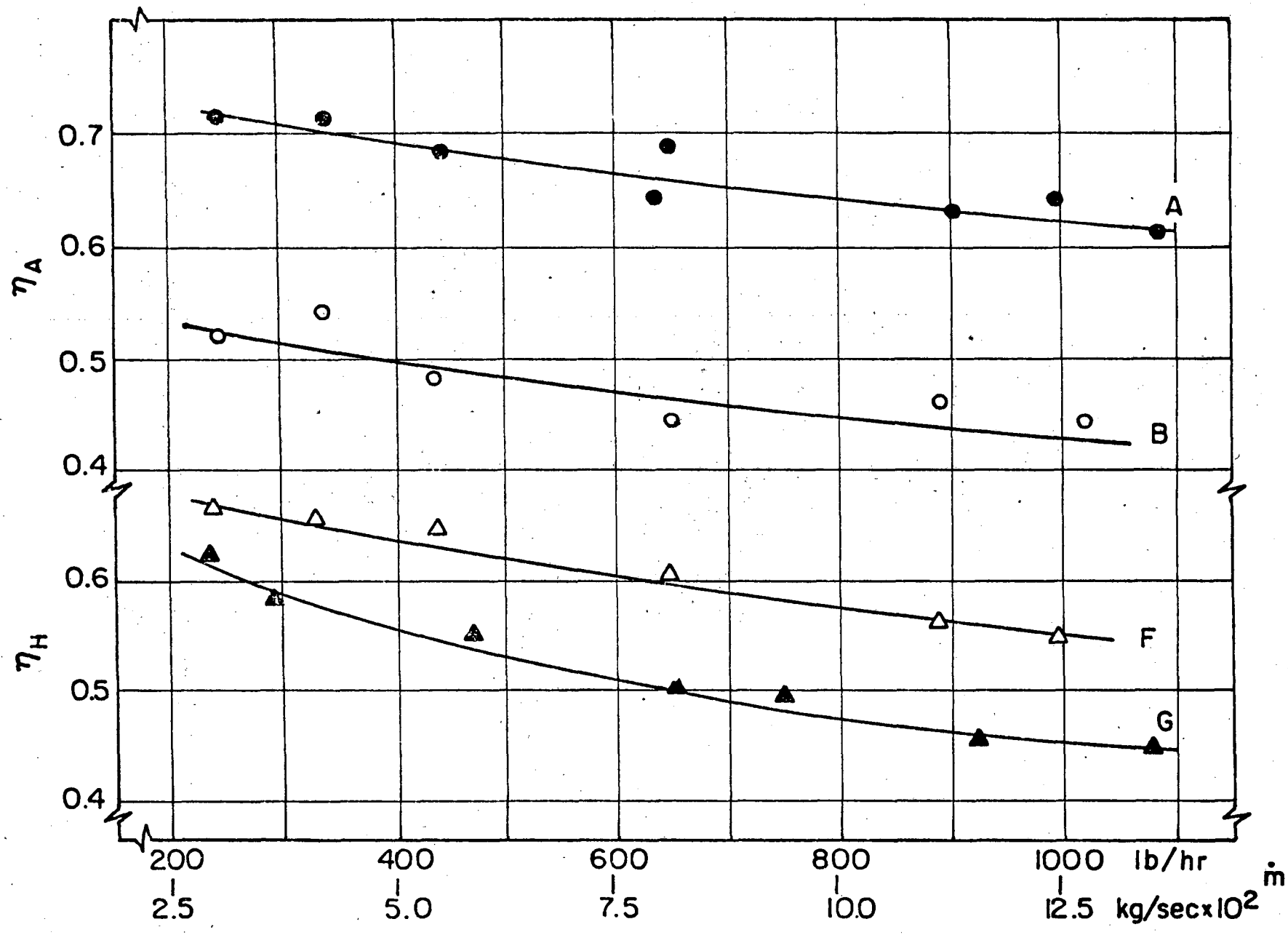

Figure 2. Experimental Effectiveness Values of G, F, B, and A Exchanger.

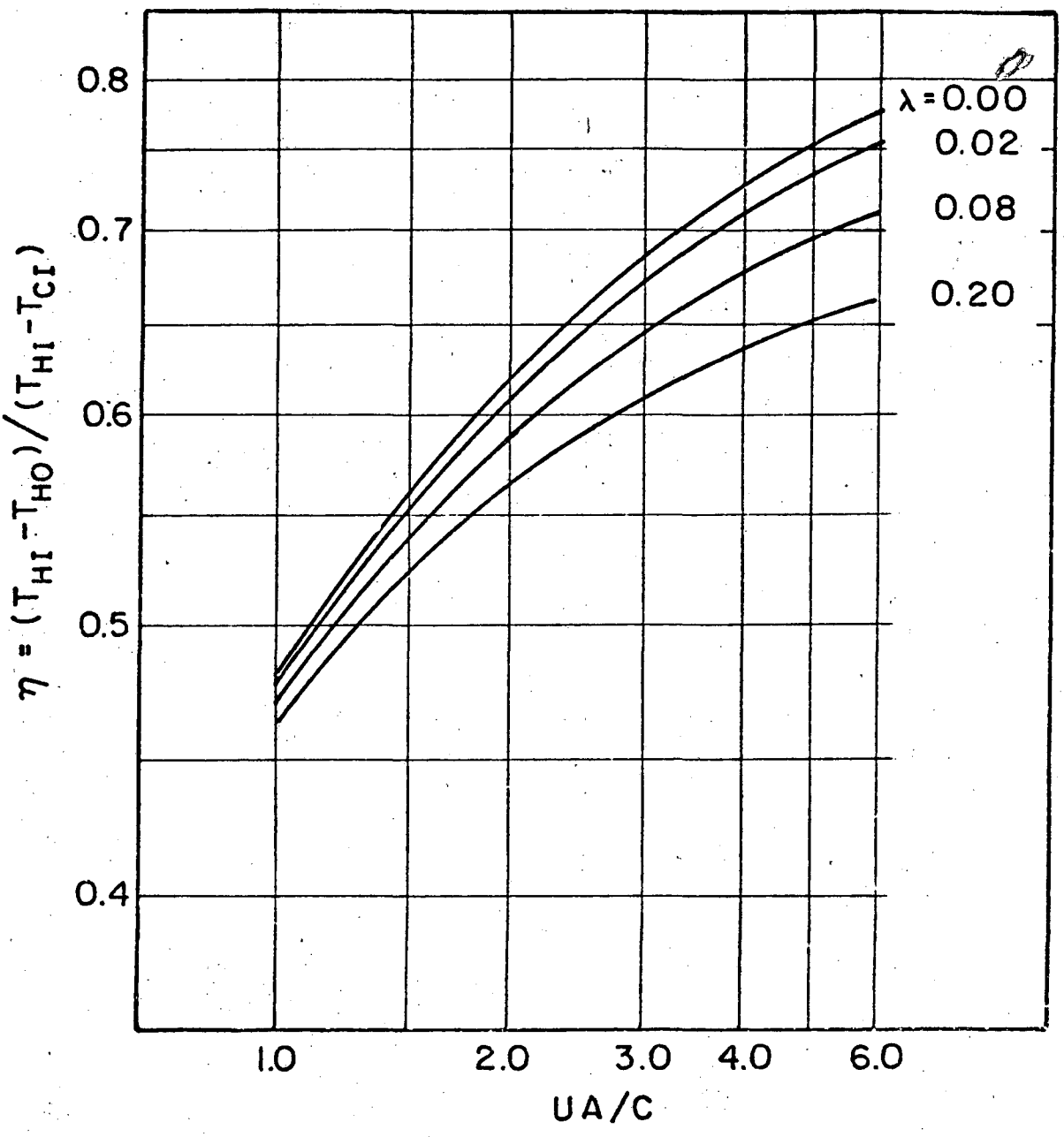

Figure 3. Theoretical Effectiveness of a Cross Flow Exchanger; Equal Longitudinal Conductivities, Equal Capacity Rates.

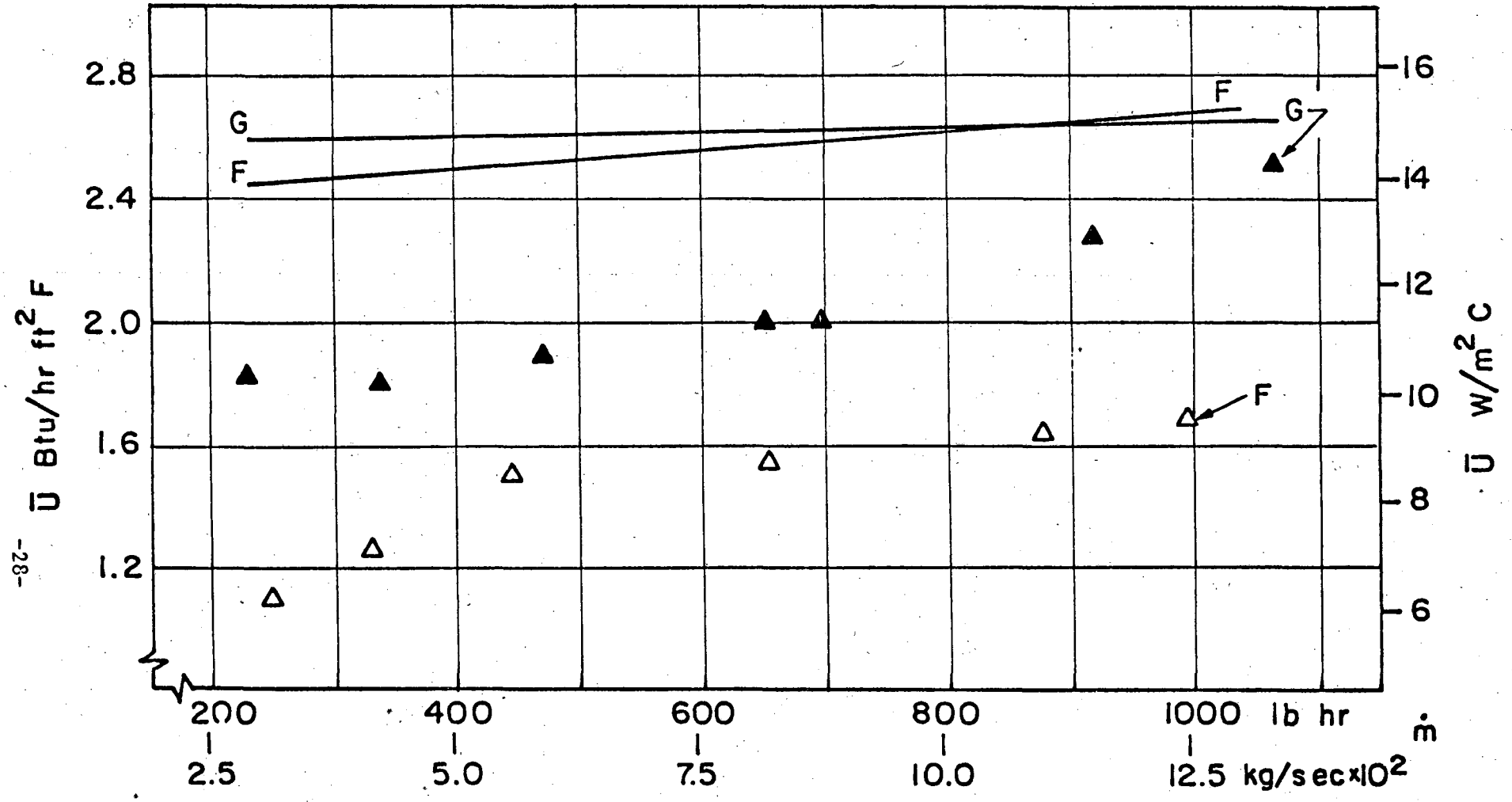

Figure 4. Experimental and Predicted Average Overall Heat Transfer Coefficients, G and F Exchangers. Curves are predictions, points are experimental values. The abscissa is $(\dot{m}_H + \dot{m}_C)/2$.

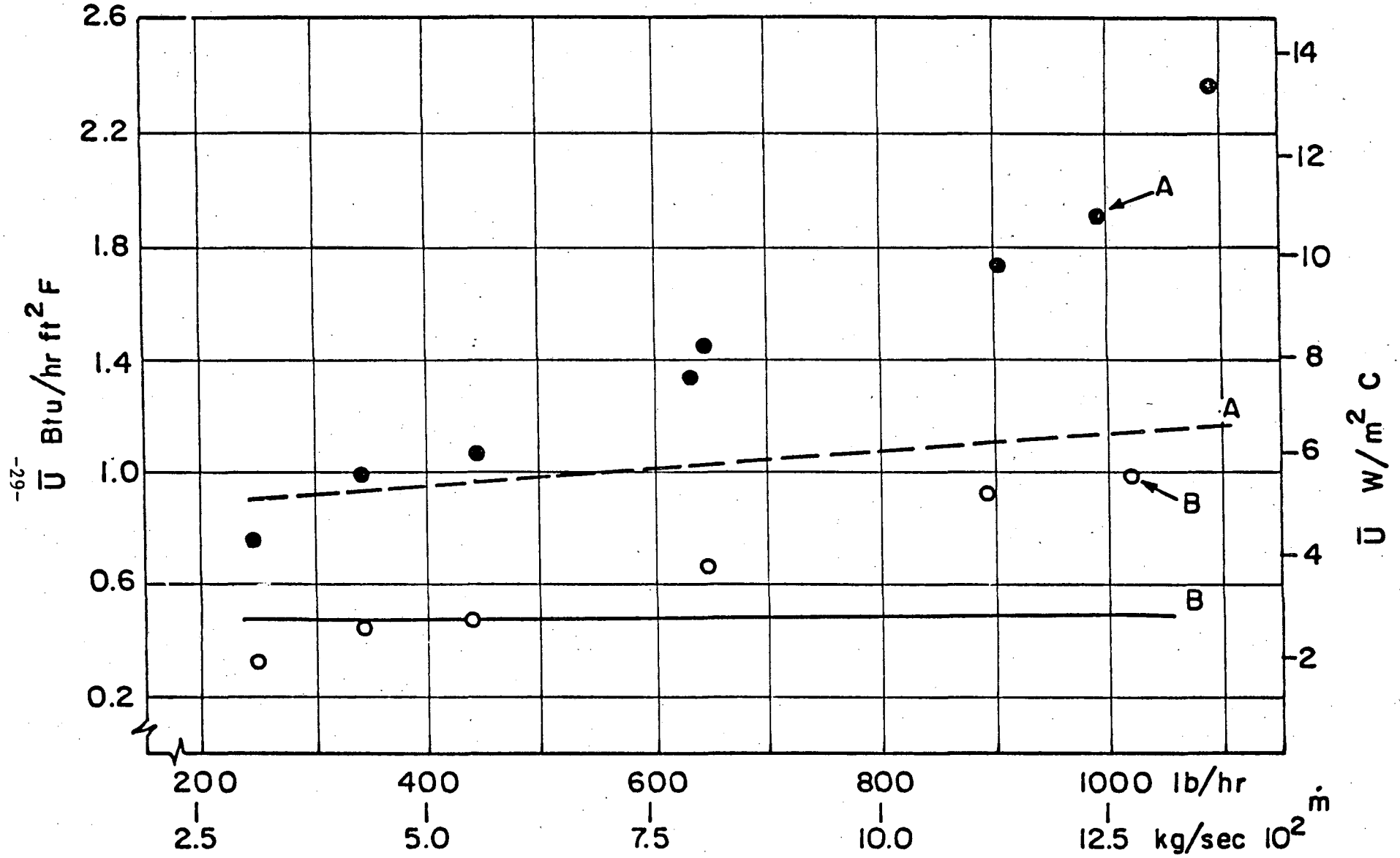

Figure 5. Experimental and Predicted Average Overall Heat Transfer Coefficients, B and A Exchangers. Curves are predictions, points are experimental values. The abscissa is $\dot{m}_H$.

TECHNICAL INFORMATION DEPARTMENT
LAWRENCE BERKELEY LABORATORY
UNIVERSITY OF CALIFORNIA
BERKELEY, CALIFORNIA 94720